sustainability

MDPI

Article

Analysis of Fault and Protection Strategy of a Converter Station in MMC-HVDC System

Chong Zhao [1], Siyu Jiang [1], Yu Xie [2], Longze Wang [1], Delong Zhang [1], Yiyi Ma [1], Yan Zhang [2,3] and Meicheng Li [1,*]

[1] State Key Laboratory of Alternate Electrical Power System with Renewable Energy Sources, School of New Energy, North China Electric Power University, Beijing 102206, China; 1152111018@ncepu.edu.cn (C.Z.); 120202211047@ncepu.edu.cn (S.J.); 1182111018@ncepu.edu.cn (L.W.); zhangdelong@ncepu.edu.cn (D.Z.); 120212211018@ncepu.edu.cn (Y.M.)

[2] School of Economics and Management, North China Electric Power University, Beijing 102206, China; 120202206223@ncepu.edu.cn (Y.X.); zhangyan8698@ncepu.edu.cn (Y.Z.)

[3] Beijing Key Laboratory of New Energy and Low-Carbon Development, Beijing 102206, China

* Correspondence: mcli@ncepu.edu.cn

Abstract: With the development of power energy technology, flexible high voltage direct current (HVDC) systems with high control degree of freedom flexibility, power supply to passive systems, small footprint, and other advantages stand out in the field of long-distance large-capacity transmission engineering. HVDC transmission technology based on a modular multilevel converter has been widely used in power grids due to its advantages such as large transmission capacity, less harmonic content, low switching loss, and wide application field. In the modular multilevel converter (MMC)-based HVDC system, the protection strategy of converter station internal faults is directly related to the reliability and security of the power transmission system. Starting from the MMC topological structure, this paper establishes the MMC mathematical model in a synchronous rotation coordinate system by combining the working state of sub-modules and the relationship between each variable of the upper and lower bridge arms of each phase of the MMC. It provides a theoretical basis for the design of the MMC-HVDC control system. The causes of the AC system faults and the internal faults of the converter station in the MMC-HVDC system are analyzed, and the sub-module faults and bridge arm reactor faults in the converter station are studied. The sub-module redundancy protection and bridge arm overcurrent protection strategies are designed for the faults, and the correctness of the scheme is verified by Matlab/Simulink.

Keywords: MMC-HVDC; protection strategy; sub-module faults; converter station; Matlab/Simulink

Citation: Zhao, C.; Jiang, S.; Xie, Y.; Wang, Y.; Zhang, D.; Ma, Y.; Zhang, Y.; Li, M. Analysis of Fault and Protection Strategy of a Converter Station in MMC-HVDC System. *Sustainability* **2022**, *14*, 5446. https://doi.org/10.3390/su14095446

Academic Editor: Domenico Curto

Received: 9 March 2022
Accepted: 28 April 2022
Published: 30 April 2022

Publisher's Note: MDPI stays neutral with regard to jurisdictional claims in published maps and institutional affiliations.

1. Introduction

With the rapid development of renewable energy generation technology, the gradual improvement of the application of new energy [1–3], and the promotion of long-distance large-capacity transmission mode, the high voltage, direct current (HVDC) transmission system has once again become a hot research and engineering application [4,5]. The good reliability and control flexibility of the voltage-source converter (VSC)-based HVDC system has been tested in the long-running process, but there are many shortcomings in the practical application of the three-phase two-level VSC-HVDC. For instance, because the level number of the two-level or three-level converter is small, the switching loss is relatively high, and there are difficulties in voltage equalization. For instance, power quality is reduced by the unstable output of renewable energy sources [6–8]. In 2001, Rainer Marquard, a German scholar, invented a new topology, and the modular multilevel converter stepped into the field of HVDC power transmission [9–11]. The modular multilevel converter (MMC)-based HVDC system has some characteristics better than VSC-HVDC, for

example [12,13], as the switching frequency of the converter is reduced, the output voltage waveform is more stable, and the quality of frequency waveform is relatively improved because the structure of MMC realizes the output characteristic of multi-levels [14,15]. In a word, the emergence of a new topology improves the operational performance of the converter on the whole. In addition to the above characteristics, MMC-HVDC technology is also applied in a wide range of fields, such as grid connection of new energy, asynchronous interconnection of regional power grids, multi-terminal DC power transmission, and the formation of DC power transmission and distribution grids in large and medium-sized cities [16–18]. Therefore, research on the MMC-HVDC topology structure, mathematical modeling, parameter selection, vector control strategy, system behavior, and protection strategy in case of failure of the converter station will play a crucial role in engineering application and analysis [19].

In flexible DC transmission, the AC systems are independent of each other. When one party cannot work normally, the other party can operate normally. If a scientific and reasonable control method can be given to the corresponding system, the overcurrent in the system can be reduced and the stability of the system can be effectively maintained. Flexible HVDC control strategies can be classified into the following two categories: (1) Direct control strategy: its strategy adopts an indirect current control mode, which will make the current response speed of its AC side low but it is difficult to realize overcurrent control. Therefore, this control strategy is seldom used in practical projects. (2) Vector control strategy: In vector control, the voltage and current in the three-phase static coordinate system are transformed to the D-Q synchronous rotating coordinate system through coordinates, and then the modulation situation and phase angle output value in the MMC-HVDC system are controlled by controlling the AC voltage and current flowing through the converter reactor. The dynamic performance of vector control and its ability to control overcurrent are the important advantages that make it widely used in HVDC flexible transmission projects. This control mode is mainly adopted in this paper, that is, the rectifier station of the converter system adopts the control mode of the outer ring's constant active power and constant reactive power to match the inner ring's constant current, and the inverter station of the converter system adopts the control mode of the outer ring constant DC voltage and constant reactive power to match the inner ring constant current.

Based on the structure and protection policies of the MMC-HVDC system, the faults of the MMC-HVDC system are divided into three parts: the internal fault, AC system fault, and DC line fault [20–23]. The conventional AC side fault removal method is proposed in [24], ignoring the internal operation mechanism of the sub-module. Document [25] focuses on the development of new sub-modules, however, the calculation, control revision, and correction of half-bridge sub-modules in existing projects are not considered. So this approach is not practical. The works in [26] put forward sub-module deployment-level control and system-level control of the MMC-HVDC system based on the electromagnetic transient model of the MMC-HVDC system, but the bridge arm reactance in the modeling and control is not under consideration. Reference [27] analyzes the characteristics and mechanisms of DC line faults and proposes corresponding control and protection principles for different types of DC line faults. However, the description of the characteristics and mechanism of line faults is rather vague. References [28–31] studied the dynamic characteristics and control of the MMC-HVDC system under the condition of a grid balance and unbalance operation.

The works in [32] compare the performance differences between VSC-HVDC and MMC-HVDC in detail from symmetric and asymmetric faults. Reference [33] proposed a multi-terminal MMC-HVDC system, and the control flexibility and reliability were analyzed. Aiming at the problem of the DC side fault of the multi-terminal HVDC system based on MMC, the literature [34] proposed a method to reliably remove the DC fault terminal using a hybrid DC switch. A resonant hybrid DC circuit breaker for multi-terminal HVDC systems was proposed in [35] which did not study the interior of sub-modules (SMs). The existing control methods are based on the premise that the number of SMs per

phase remains unchanged, and redundant SMs are difficult to play a role. Since the MMC models established at present are all based on the change of sub-module topology, the research on a redundancy strategy for existing sub-modules needs to be carried out. A mutual-inductance-type fault current limiter (MFCL) using coupled reactors and few power electronic switches is proposed. Compared with the conventional DC reactors, it can automatically limit the fault current during the current rising stage with an increased equivalent inductance and accelerate the decline of the current by reducing the inductance of the discharge circuit [36]. The resonance of modular converter is studied by cell partition [37].

Despite existing studies, several aspects still need to be improved in this research field. Firstly, most of the research is too general to analyze the internal faults of the converter station and the asymmetric faults of the AC system, and unable to analyze the faults in detail according to practical situations. Moreover, the sub-module inside the converter station is the main equipment, which is directly related to the steady and dynamic performance of the converter station. Once the sub-module fails, the redundancy protection of sub-modules should be taken into consideration. The bridge arm reactor is the power transmission link between MMC and AC systems. There is a research gap in the bridge arm overcurrent protection strategies.

Based on the existing research, we propose setting a certain number of hot standby sub-modules and cold standby sub-modules in each bridge arm. The causes of the AC system fault and internal fault of the converter in the converter station of the MMC-HVDC system are analyzed. The sub-module fault and bridge arm reactor fault in the converter station are studied. For the faults, innovative sub-module redundancy protection and bridge arm overcurrent protection strategies are designed, and the correctness of the scheme is verified. Compared with existing studies, the main contributions of this study can be summarized as follows:

(a) This paper proposes to set a certain number of hot standby sub-modules and cold standby sub-modules in each bridge arm.
(b) The causes of the AC system fault and internal fault of the converter in the converter station of the MMC-HVDC system are analyzed.
(c) The sub-module fault is studied. For the fault, innovative sub-module redundancy protection is designed, and the correctness of the scheme is verified.
(d) The bridge arm reactor fault in the converter station is studied. For the fault, innovative bridge arm overcurrent protection strategies are designed, and the correctness of the scheme is verified.

The remainder of this paper is organized as follows. According to the relationship between the number of faulty sub-modules and the number of redundant sub-modules, the corresponding sub-module redundancy protection strategy is proposed in Section 2. Section 3 analyzes the reasons for the bridge arm reactor failure in the converter station of the MMC-HVDC system. Finally, Section 3 simulates the change of inductance value caused by reactor failure on the RT-LAB simulation platform.

2. The Establishment of the MMC-HVDC Mathematical Mode

2.1. MMC Topology

The most important feature of the modular multilevel converter is that it has many series sub-modules, which are arranged in groups called bridge arms [38]. Figure 1 shows the topological structure of the three-phase modular multilevel converter. The upper and lower bridge arms together are called one phase, so there are six bridge arms in three phases. The upper and lower ends of one phase are connected to the DC system, and the three-phase AC system is connected to the midpoint of each phase (A, B, and C) respectively. In general, the bridge connected to the positive pole of the power supply is called the "upper arm", and vice versa, the bridge arm connected to the negative pole of the power supply is called the "lower arm". Each bridge arm consists of N sub-modules (SM)

and the bridge arm impedance series [39]. The bridge arm acts as a filter inductor, it produces equal and opposite harmonic voltage, limiting current caused by transient voltage difference sub-modules, weakening the higher harmonics in the bridge arm current, short-circuit fault current in DC lift restrictions is at a very low level, with AC harmonic voltage offset bridge arm, and steady DC voltage.

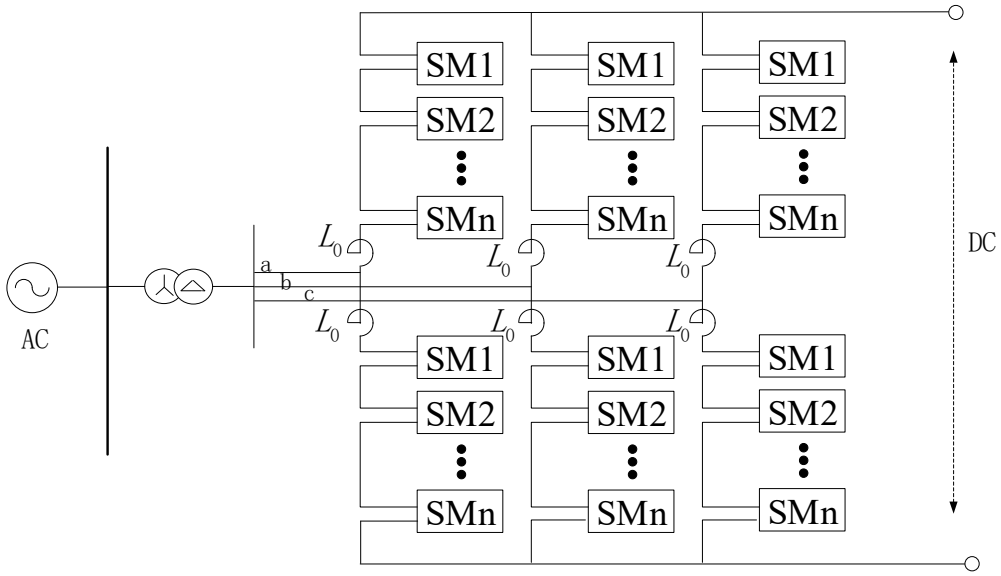

Figure 1. The topological structure of the three-phase modular multilevel converter.

The topological structure of the MMC is composed of two identical sub-module structures, the upper and lower arms which have symmetry [40,41]. To ensure the equalization of active power and reactive power, it is necessary to make the AC voltage output points of the upper and lower bridge arms of each phase equal, that is, the AC output voltage of the upper and lower bridge arms of each phase with equal potential point connected to the AC system, then this point is the potential reference point of the AC neutral point. Due to the modular design, the dynamic characteristics of the sub-modules on each bridge arm are the same, so each bridge arm can be equivalent to an equivalent sub-module, that is, the output voltages of six bridge arms can be equivalent to six controlled voltage sources.

Due to the symmetry of the three phases, the DC is evenly distributed among the three phases, that is, the DC flowing through each bridge arm is Idc/3. Because the upper and lower arms are complementary and symmetrical, the AC flowing in each arm is half of the phase current. The current contained in each bridge arm is "DC" plus "AC" plus/minus "interphase current" due to circulation.

Several topological structures of sub-modules have been mentioned in previous studies, among which the most common are full-bridge and half-bridge. The half-bridge sub-module can only generate zero voltage and positive voltage, so the DC voltage component is inevitable in the bridge arm, the half-bridge sub-module is selected only when the MMC is connected to the DC system. The full-bridge sub-module can generate both zero voltage and positive voltage as well as a negative voltage. Therefore, this sub-module can be connected to both AC and DC systems. Because there are only two switches in the half-bridge sub-module, the number of components is less and the work efficiency is higher, while the full-bridge sub-module needs to use more components.

Because the half-bridge type is more widely used, the half-bridge type sub-module is selected in this paper. The topological structure of the half-bridge sub-module is shown in Figure 2, each sub-module consists of two IGBTs (T1, T2), two diodes in reverse parallel (D1, D2), and a capacitor C. T1 and D1 are in parallel, T2 and D2 are in parallel, and the two groups are connected in series. The capacitors are in parallel at both ends.

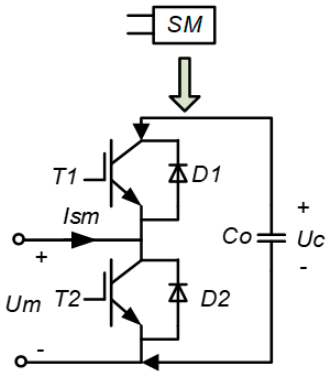

Figure 2. The topological structure of the half-bridge sub-module.

2.2. How MMC Works

When the MMC acts as a rectifier, the left three-phase is connected to the AC power supply, and the AC flows through the inductance into each sub-module in the bridge arm. The DC voltage is the output at the DC side through the constant change of the sub-module input and the number of cuts. When MMC acts as an inverter, DC voltage sources with equal voltage values are connected to the upper and lower bridge arms, respectively, which are Vdc/2. The DC voltage flows to the AC side through the sub-module, and the three-phase sinusoidal AC voltage is the output. The amplitude difference of each phase is 120 degrees [42].

By controlling IGBT on or off, each sub-module has three different working states, namely input state, excision state, and locked state. Due to the different directions of current flow in and out, in Table 1, the three working states can be subdivided into six working modes. Among them, the input state and the excise state are normal working states, and the locked state is only used when the pre-charging or DC fault is started. The output voltage of the sub-module is controlled by triggering and shutting off the fully controlled device.

Table 1. Working status and the current path of the modular multilevel converter (MMC) sub-module.

Working Status of the Sub-module	Switch State	Current Path Circuit
Locked state	VT1 Shut off	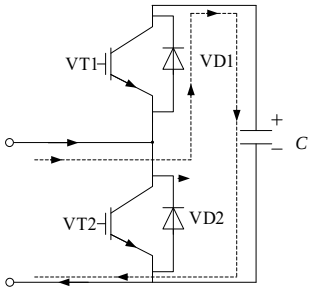
	VT2 Shut off	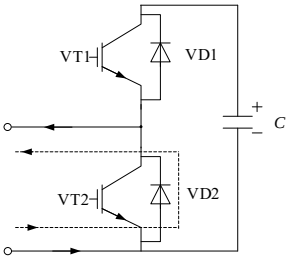

Input	VT1 conduction	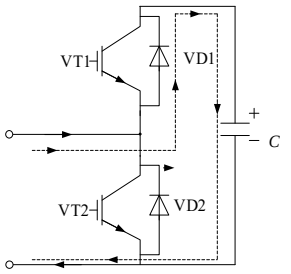
	VT2 Shut off	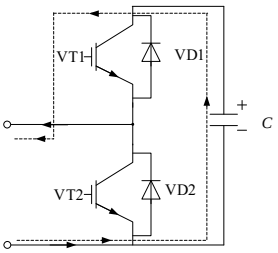
Excise	VT1 Shut off	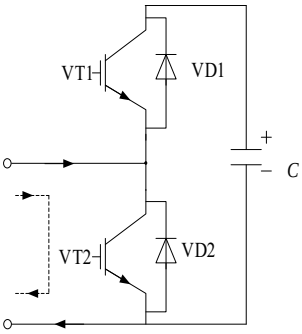
	VT2 conduction	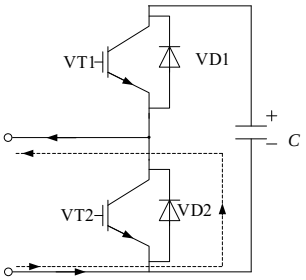

Locked state: T1 and T2 are in the off state

(1) Charging mode: current flows in from A, passes through diode D1, flows through capacitor forward, and flows out from B. The capacitor is then plugged into the circuit and charged.

(2) Bypass mode: current flows in from B, passes through diode D2, and flows out from A. The capacitor is not connected to the circuit and is in a bypass state.

Input state: T1 open, T2 off

(3) Discharge mode: current flows in from B, flows through the capacitor in reverse, passes through conduction T1, and flows out from A. The capacitor is then plugged into the circuit and discharged.

(4) Resection status: T1 resection and T2 opening

(5) Bypass state: when the current flows in from A, it flows out from B through conducting T2. The capacitor is not connected to the circuit and is in a bypass state.

(6) Bypass state: when the current flows in form B, it passes through diode D2, and flows out from A. The capacitor is not connected to the circuit and is in a bypass state.

If N sub-modules are on in each phase, the capacitance-voltage of each sub-module is U_{dc}/N. The output level is changed by changing the number of sub-modules input by

the upper and lower bridge arms. The output level is equal to the number of sub-modules on each bridge arm plus one, that is, if there are N sub-modules in each phase, the output level is $N/2 + 1$.

In this paper, the mathematical model is analyzed from the point of view of the rectifier side of the system. The circuit structure diagram of the rectifier side of the MMC is shown in Figure 1.

U_g is the AC voltage at the outlet of the converter, U_{dc} is the DC side voltage of the converter, U_u and U_p are the voltage of the upper and lower bridge arms, I_u, I_p, I_g, and I_c are the current of the upper bridge arm, the current of the lower bridge arm, the phase current of the AC port and the internal circulation, L and R are the inductance and equivalent resistance of the bridge arm respectively. The bridge arm resistor can simulate the power loss inside each bridge arm of the MMC.

The relationship among the upper bridge arm current I_u, lower bridge arm current I_p, AC port phase current I_g, and internal circulation I_{cir} can be expressed as follows:

$$I_g = I_p - I_u \tag{1}$$

$$I_{cir} = \frac{I_u + I_p}{2} \tag{2}$$

The relationship between the voltage of upper bridge arm U_u, the voltage of lower bridge arm U_p, common-mode voltage of upper and lower bridge arm U_{com} and differential mode voltage of upper and lower bridge arm U_{diff} can be expressed as follows:

$$U_{diff} = -\frac{1}{2}(U_p - U_u) = \frac{1}{2}(U_u - U_p) \tag{3}$$

$$U_{com} = \frac{1}{2}(U_u + U_p) \tag{4}$$

According to Kirchhoff's voltage law (KVL), the circuit equation can be listed:

$$\frac{1}{2}U_{dc} - U_u - L_{arm}\frac{dI_u}{d_t} - R_{arm}I_u = Ug \tag{5}$$

$$-\frac{1}{2}U_{dc} + U_p + L_{arm}\frac{dI_p}{d_t} + R_{arm}I_p = Ug \tag{6}$$

When the sub-module is in the input state, the output voltage of the sub-module is the capacitor voltage, and when the current is positive, the capacitor charges, and the capacitor voltage increases. When the current is negative, the capacitor discharges and the capacitor voltage decreases. When the sub-module is removed, the capacitor is not used and the output voltage of the sub-module is 0. The input and excision states of sub-modules are represented by switching functions.

The control of a single MMC [30] converter station in a multi-terminal HVDC transmission system is generally divided into three layers: system-level control, converter station level control, and valve level control. System-level control generates P_{ref}, Q_{ref}, U_{acref}, U_{dcref}, and other reference values of each active and reactive power class control, which are transmitted to the converter station level control layer. Then the station level control receives the setting values of system-level control to generate modulation ratio and phase shift angle signals, which are transmitted to the valve level control layer, finally achieving the control goal.

First of all, the current and voltage output values are input to the master controller, and the reference value of the control quantity is input to the master controller. The master controller performs a d-q decoupling transformation to generate the required modulation wave and transmits it to the modulation part. Secondly, the modulation part receives the

modulation wave signal sent by the main controller and adopts the modulation strategy of nearest level approximation to calculate the number of sub-modules that need to be turned on for each bridge arm. Then, according to the number and voltage of the conduction, the sub-module capacitor voltage balances control, usually by using the sequencing method at the same time the modulation part needs to suppress the circulation. Finally, the modulating part transmits the modulating signal to the sub-module to generate the corresponding trigger pulse and control the IGBT on or off. The equivalent circuit of the system in the synchronous rotation coordinate system can be obtained, as shown in Figure 3, as the equivalent circuit of the system in the d-q synchronous rotation coordinate system. Figure 3.

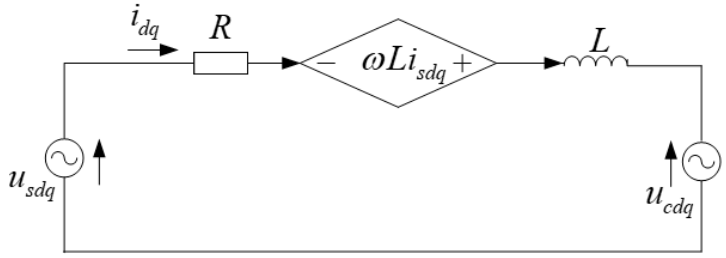

Figure 3. Equivalent circuit of the system.

To facilitate the design of the control level controller of the MMC-HVDC system, the mathematical model obtained in the frequency domain is shown in Figure 4. The flexible DC transmission system adopts a double closed-loop control strategy to control the active power and reactive power in the system, the outer loop adopts constant voltage control, and the inner loop adopts current control. The circuital model in the frequency domain of the MMC is shown in Figure 5.

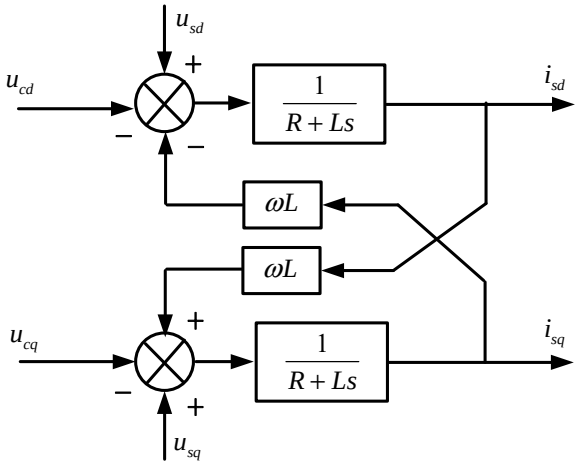

Figure 4. Outer loop control diagram of MMC-HVDC system.

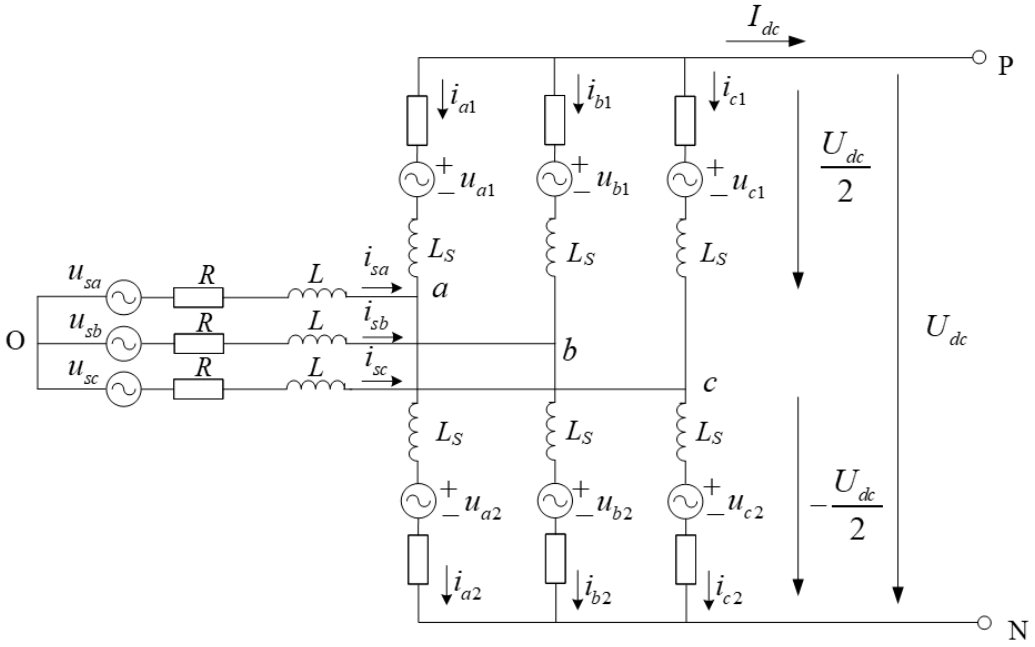

Figure 5. MMC-HVDC system converter station.

2.3. MMC Modulation Method

The recent level approximation modulation strategy is based on the continuous adjacent voltage instantaneous value correction. To decide on the moment, the bridge arm should input the number of modules to change the number of sub-modules, generated from the lowest to the highest voltage square wave of different values, and this voltage superposition is based on the modulation wave approximation.

In the situation of high levels (tens to hundreds of levels), the step wave modulation can effectively solve the harmonic problem, and the output voltage waveform is of high quality. Compared with the PWM modulation technology, the nearest level approximation modulation strategy is easy to implement, requiring less calculation work, using a smaller switching frequency, and causing low switching loss.

When the number of sub-modules input by upper and lower bridge arms is equal, that is, when n/2 sub-modules are input by each phase, the output voltage of the phase is 0. With the increase in the number of input sub-modules of the lower bridge arm, the output voltage waveform increases gradually from 0 according to the rule of the sine wave, until the output voltage waveform reaches the peak value when all input is completed. At any time, due to the change in the input state of the sub-module, the square wave generating different voltage levels should be as close to the modulation wave as possible.

At each moment, when the total number of sub-modules in each phase is 2*N*, the number of sub-modules needed by the upper and lower bridge arms N_u and N_p are respectively:

$$\begin{cases} N_p = N + round\left(\dfrac{U_s}{U_c}\right) \\ N_u = 2N - N_p = N - round\left(\dfrac{U_s}{U_c}\right) \end{cases} \tag{7}$$

where, U_s represents the voltage instantaneous value of the modulated wave, and U_c represents the average value of capacitor voltage of all sub-modules on a phase bridge arm.

Round(x) is the nearest rounded function, taking the nearest integer to x. For example, if U_s/U_c = 5.2, invest 5 sub-modules; if U_s/U_c = 5.8, invest 6 sub-modules.

2.4. Internal Circulation Suppression Strategy

Due to the existence of voltage difference between three-phase bridge arms, internal circulation appears in the MMC three-phase bridge arms, which contain a negative sequence component with a frequency twice the fundamental frequency. The internal circulations do not affect the AC side voltage and current, but if not properly suppressed, they increase the peak and root mean square values of the current of each phase bridge arm, thereby increasing the power loss of the converter and the ripple magnitude of the submodule capacitance voltage. Although the internal current can be suppressed to some extent by properly adjusting the size of the bridge arm inductance, the internal circulation suppression strategy is still necessary.

Due to internal circulation, the current contained in each bridge arm is "DC" plus "AC" plus/minus "interphase circulation". Therefore, the bridge arm voltage is "DC voltage" plus "voltage fundamental wave component" plus "double frequency fluctuation component". The second frequency wave component satisfies the following formula:

$$\begin{cases} U_{2\,fa} = \rho \cdot L_{arm} I_{2\,fa} + R_{arm} I_{2\,fa} \\ U_{2\,fb} = \rho \cdot L_{arm} I_{2\,fb} + R_{arm} I_{2\,fb} \\ U_{2\,fc} = \rho \cdot L_{arm} I_{2\,fc} + R_{arm} I_{2\,fc} \end{cases} \tag{8}$$

where U_{2fi} is the fundamental wave component of double frequency, I_{2fi} is the interphase circulation, P is the differential operator, and L_{arm} and R_{am} are the equivalent reactance and resistance.

Because the nature of the circulation is the double frequency negative sequence component, the formula coordinates are converted to the double frequency negative sequence rotating coordinate system to realize the quantitative control of the circulation.

$$\begin{cases} U_{2\,fd} = \rho \cdot L_{arm} I_{2\,fd} + R_{arm} I_{2\,fd} - 2L_{arm} I_{2\,fq} \\ U_{2\,fq} = \rho \cdot L_{arm} I_{2\,fq} + R_{arm} I_{2\,fq} + 2L_{arm} I_{2\,fd} \end{cases} \tag{9}$$

I_{2fd} and I_{2fq} are the D and Q axis components of the interphase circulation in the double frequency negative sequence rotation coordinate system respectively. According to this equation, a mathematical model of internal circulation can be obtained, as shown in the figure below.

As shown in Figure 6, the interphase circulation is converted into the DC components of the d and q axes in the double frequency negative sequence rotation coordinate system, and the difference between their measured values and their reference values is input to the PI controller. Cross-coupling control is adopted. When the d-axis component of the circulation is controlled by PI, the Q-axis component of the circulation suppression voltage is obtained by adding the voltage on the Q-axis resistor. When the q-axis component of the circulation is controlled by PI, the D-axis component of the circulation suppression voltage is obtained by adding the voltage to the D-axis resistance. The additional voltage signal to suppress the circulation can be obtained by inverse coordinate transformation, and this signal can be superimposed on the reference value of each phase voltage to suppress the circulation in the MMC. The following equation is the mathematical model of internal circulation suppression under the transformation of the double frequency negative sequence coordinate system.

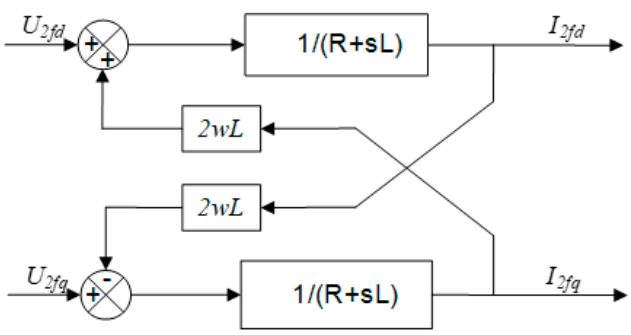

Figure 6. Internal circulation suppressor control block diagram.

$$\begin{cases} U_{2\,fd} = -2L_0\left(K_p + \dfrac{K_i}{s}\right)\left(I_{2\,fqref} - I_{2\,fq}\right) + R_0 I_{2\,fd} \\ U_{2\,fq} = -2L_0\left(K_p + \dfrac{K_i}{s}\right)\left(I_{2\,fdref} - I_{2\,fd}\right) + R_0 I_{2\,fq} \end{cases} \quad (10)$$

Among them, I_{2fd} and I_{2fdref} are the reference values of the internal circulation, and the reference values should be set to 0 to suppress the circulation.

3. Analysis of Internal Fault Characteristics of the Converter station

3.1. Fault Analysis of MMC Sub-Module

The sub-module is composed of controllable turn-off power electronic devices, diodes, and capacitors. Once one of the three devices fails, the sub-module will fail. If there is no input of corresponding control and protection strategy, the converter will enter an abnormal working state and will exit from operation if it is serious.

If the sub-module is faulty, different working states of the sub-module have different solutions. If the faulty sub-module is removed, the system will be not affected. When the fault sub-module is locked, the system will not be affected as long as the fault sub-module is not put in. When the fault sub-module is in the input state, the number of ongoing sub-modules will be less than N, resulting in the voltage sag of the bridge arm, which is insufficient to support the DC voltage. In this way, the voltage difference between the fault phase and the other two phases will lead to the emergence of phase circulation. At this point, we need to eliminate the faulty sub-module and put in a new redundant sub-module. Therefore, when a small number of sub-modules fail, we need to add the control strategy of sub-module protection into the control system to ensure the smooth operation of the converter and enhance its reliability. The specific parameters of the simulation model are in Table 2.

Table 2. The specific parameters of the simulation model.

The voltage level of the main network on both the rectifier side and the inverter side	220 kV
The Ynd type is connected to the converter transformer with the longitude ratio	220/230 kV
The ac rated bus voltage	230 kV
The number of sub-modules of each bridge arm of MMC	N = 30
The inductance value of the reactor on each bridge arm	70 mH
The equivalent resistance of the system	0.1 ω
The rated DC voltage	±230 kV
The rated transmission active power	1200 MW

The reactive power	480 MVA

Using the MMC-HVDC system model established above, the sub-module failure is simulated and verified without adding the sub-module protection strategy. At 7.1 s, the setting failure occurs, and one of the sub-modules of the upper bridge arm of phase A on the rectifier side fails.

As can be seen from Figure 7, Figure 7a three-phase AC simulates the three-phase voltage on the AC side, and the fault occurs in 7.1 s. The current at the time of single-phase fault is corresponding to three-phase AC. Due to the failure of a sub-module of phase A and insufficient voltage of the bridge arm, the three-phase circuit is asymmetric, the three-phase AC of the system oscillates seriously, waveform distortion occurs, and a large amount of circulation occurs. Therefore, even if a sub-module fails, it will still have a great impact on the system in the absence of protection policies. We should adopt an appropriate redundancy protection control strategy, in the case of sub-module failure, cut off, and put in a new sub-module to replace the faulty sub-module so that the converter station can maintain a normal steady operation.

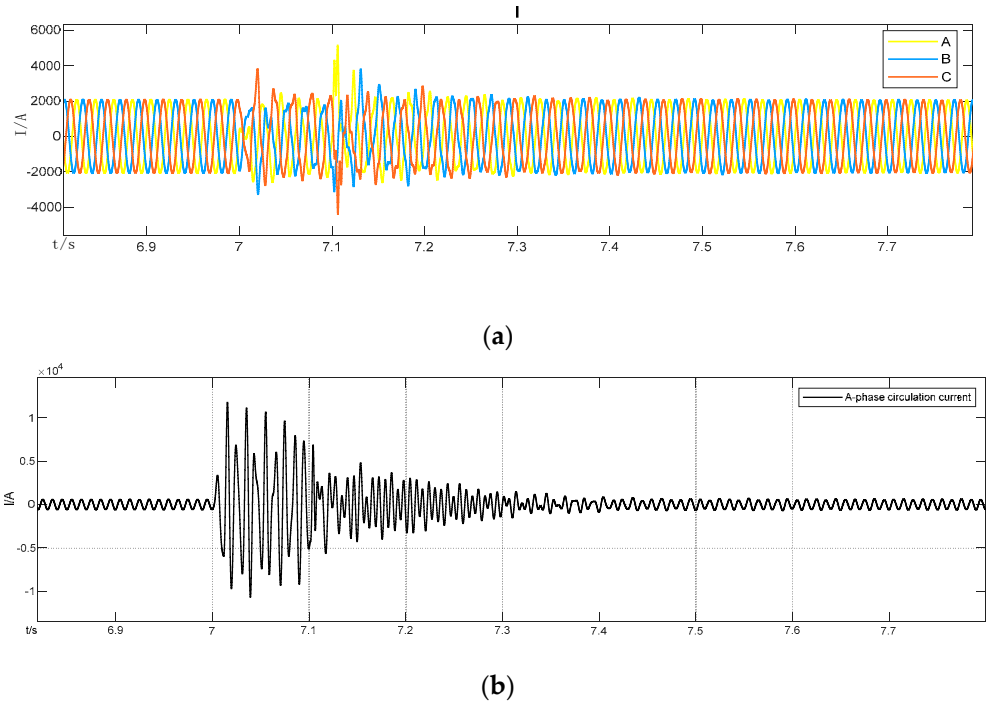

Figure 7. Rectifier station system two waveforms after sub-module fault removal. (**a**) is Three-phase AC; (**b**) is A-phase circulation current.

3.2. Fault Analysis of Bridge Arm Reactor

The bridge arm reactor is connected in series on each bridge arm. As a bridge between the MMC and the AC system, it can not only suppress the ripple of output voltage and current, making the output voltage and current close to the ideal value, but also limit the short-circuit current. Therefore, the failure of the bridge arm reactor should be prevented to ensure the stable operation of the MMC-HVDC system. However, the probability of the bridge arm reactor inter-turn short circuit is very high. Once the inter-turn insulation of the bridge arm reactor is destroyed, resulting in an inter-turn short circuit fault, the device will heat and the inductance value will decline, leading to increased circulation, harmonic generation, and oscillation phenomenon. In serious cases, an excessively high temperature may lead to a breakdown phenomenon, which will make the reactor fail.

Using the MMC-HVDC system model established above, the bridge arm reactor failure is simulated and verified. The inductance value changes due to the failure of the simulated reactor. When the bridge arm reactor is set to fail for 1 s, the inductance value of the bridge arm decreases from 70 mH to 60 mH in phase A, the simulation results are shown in Figure 8.

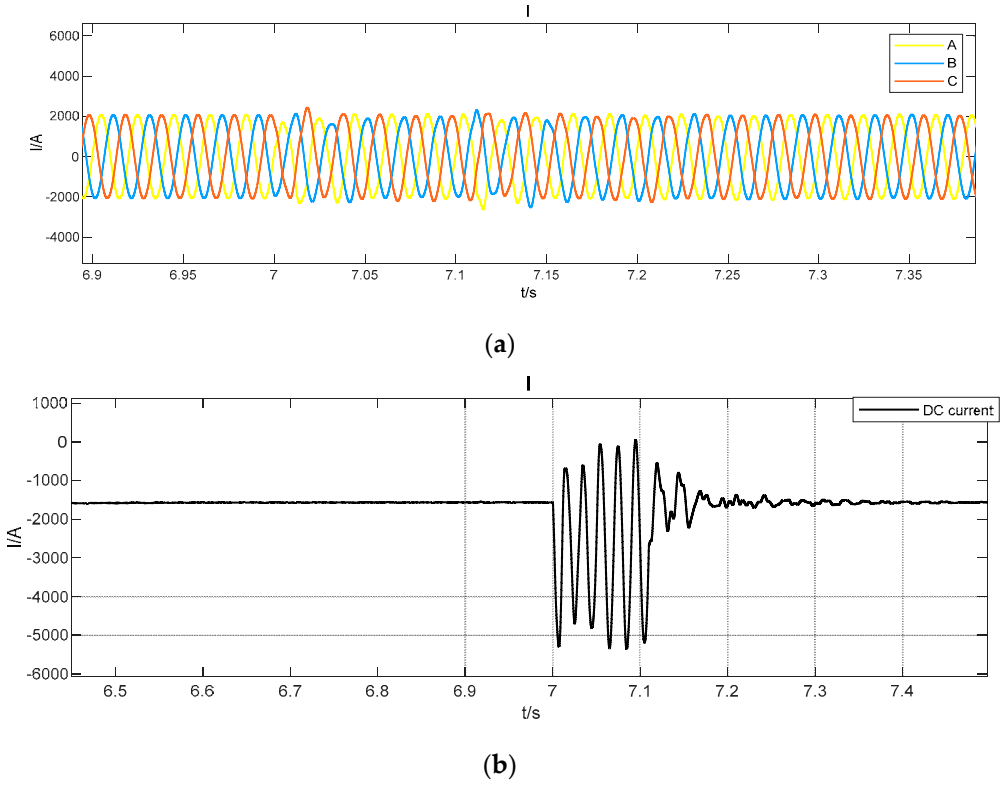

Figure 8. System simulation results when the reactor fails. (**a**) Three-phase AC current; (**b**) DC current.

As can be seen from the simulation results in Figure 8, when a fault occurs at 7 s, the reactance value decreases, and its ability to suppress ripples decreases, resulting in unbalanced three-phase AC and waveform distortion, which leads to the increase and shock of DC voltage. In analyzing the reactor failure for the bridge arm, its failure directly affects the stable operation of the system, and cannot be contained, which, therefore, can be classified as a permanent fault. Once the fault is detected, the converter station should be locked immediately. At the same time, the AC circuit breaker is tripped to make the system stop running, and then the reactor bridge arm is repaired. After maintenance, it is put into operation in the system after passing the test.

3.3. Analysis of Converter Station Protection Strategy

Aiming at the sub-module fault mentioned above, this paper proposes the sub-module redundancy protection strategy. The upper and lower bridge arms of each phase of the MMC are respectively equipped with standby sub-modules. When the sub-modules of the whole system do not fail and run normally, the standby sub-modules are in the standby state and are not put into the system to realize charging and discharging operations. If a sub-module fails in the entire system, the redundant protection policy is enabled to remove the faulty sub-module from bypass mode, and the standby sub-module is immediately put into operation to replace the faulty sub-module so that the MMC-HVDC system can run normally. The redundancy protection strategy can not affect the normal

operation of the system, in the case of a small number of sub-modules failure, making the whole system protected without downtime and maintenance.

The redundant sub-module designed here has two states: hot standby state and cold standby state. Before the two states are put into operation, the output voltage of the sub-module is 0.

The hot standby state child module is the sub-module that is in a normal working state of resection. If the sub-module in the system fails, to prevent abnormal operation of the whole system caused by the impact of a large area, the redundant modules should be guaranteed speediness, so the hot standby module on the disconnect bypass switch K1 can quickly put into operation the fault module. The bypass switch K1 of the sub-module in the cold standby state is closed, and the sub-module is in the state of being bypassed. IGBT switch tubes VT1 and VT2 are off, so no current flows and no voltage drop is generated. If a system is full of sub-modules in the hot standby state, the running speed of the system will be reduced and the loss of the system will be increased. Therefore, the input redundancy protection control strategy for the MMC-HVDC system should set redundant sub-modules for each bridge arm, one part of which is the hot standby sub-module, and the other part is the cold standby sub-module. On the premise that the original operating state of the system is not changed: the sub-modules of each phase input remain unchanged and can well support the DC voltage, the redundancy protection scheme is as follows:

(1) When the sub-module running in one of the bridge arms fails, the system starts the protection strategy through signal detection, then bypasses the faulty sub-module and sends a locking signal to the faulty sub-module. At the same time, the sub-module in the hot standby state is put into use and sends a pulse signal to it, that is, to put it into a normal operation state;
(2) If the number of fault modules is over the hot standby state of sub-modules, or hot standby module failure cannot be put into operation, the cold standby module will be started, and the first child module of the cold standby state bypass switch will be turned on, making its fault module, the module running in for participation in the stable operation of the whole system.

According to the redundancy protection policy proposed above and the relationship between the number of faulty sub-modules and the number of redundant sub-modules, the redundancy protection process of the MMC-HVDC system is divided into the following situations, as shown in the Figure 9: Assume that the number of sub-modules on each bridge arm is $N + N_1 + N_2$, where the number of redundant modules is $N_1 + N_2$ which indicates the number of hot standby sub-modules, N_2 indicates the number of cold standby sub-modules, and $N_f(t)$ indicates the number of faulty modules.

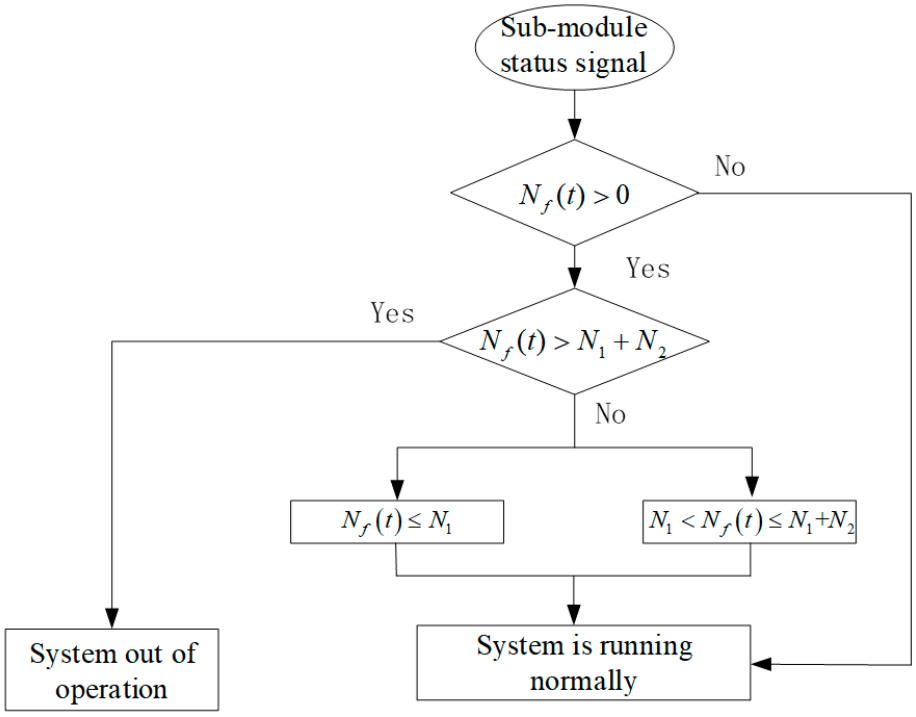

Figure 9. Flow chart of the sub-module redundancy protection strategy.

Using the MMC-HVDC system model established above, the proposed sub-module redundant protection strategy is added to verify the effectiveness of the protection strategy. On the upper and lower bridge arms of each phase, 33 sub-modules are set, namely SM1-SM33. When the system runs stably, 30 modules are put into each phase, the other 3 sub-modules are redundant, and the output voltage is 31 levels. Configure two hot standby sub-modules SM31 and SM32, and one cold standby sub-module SM33. At 1.0 s, the sub-modules with two inputs of the upper bridge arm of phase A are faulty and bypassed, and the hot standby sub-modules SM31 and SM32 are immediately put into operation. At 7.1 s, another sub-module SM30 in the input state of the upper bridge arm of phase A was set to fail and be bypassed. Since all the sub-modules in the hot standby state were put in and the number was not enough, the cold standby sub-module SM33 of the upper bridge arm of phase A was put in at 7.15 s. The simulation results are shown in Figure 10.

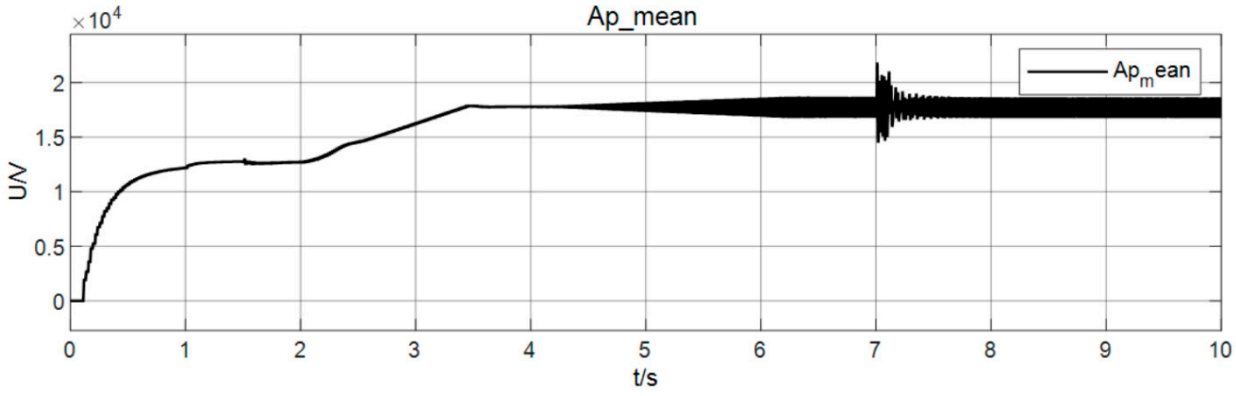

(**a**)

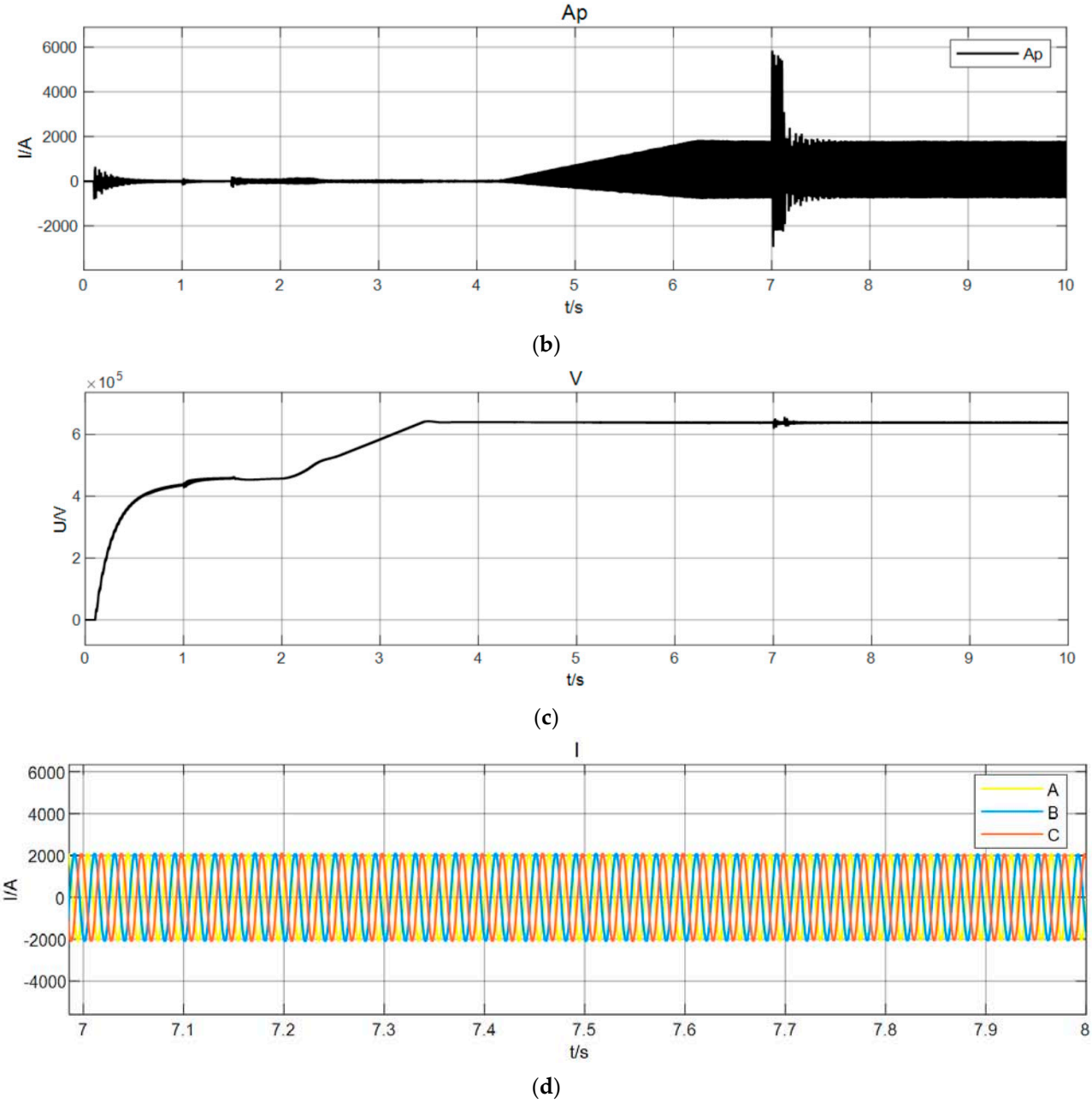

Figure 10. Sub-module Fault and Redundant Protection System Variable Waveforms. (**a**) Capacitor voltage of sub-module of upper bridge arm in phase A; (**b**) Current of sub-module of upper bridge arm in phase A; (**c**) Dc voltage; (**d**) Ac output current.

The waveform of each variable of the bridge arm on phase A of the converter station is shown in Figure 10. It can be seen that when the sub-module fails at 7 s, the input of the hot standby redundant sub-module does not affect the original normal operation of the system, because the hot standby sub-module only changes from the excused working state to the put into a working state. Therefore, the input of the bypass faulty module and the hot standby sub-module has no impact on the system operation. In 7.5 s, the sub-module fails, due to the hot standby module being fully committed, the quantity is not enough, so the cold standby module needs to be input. However, cold standby sub-modules of investment have a certain influence on the system, hence, cold standby sub-modules SM33 needs a capacitor charging process to enter a state of normal operation. The charging process is shown in Figure 10a. In the process of input, DC voltage and current oscillate, while

three-phase AC voltage and current increase and oscillate. After complete input, the system slowly enters a stable working state. Therefore, the sub-module redundancy protection strategy proposed in this paper can be applied to the case of failure of a few quantum modules, with a short recovery time and a small impact on the system.

Possible faults in the system mentioned above, such as AC single-phase grounding fault in the asymmetric short circuit, two-phase short circuit fault, and on the internal fault, DC fault, etc., will lead to overcurrent in the converter bridge arm. Once the overcurrent is not controlled in time, internal damage will be done to the power electronic device of the MMC-HVDC system. Therefore, the overcurrent protection strategy of the converter station is proposed. Usually, when the converter station is faulty and overcurrent occurs, the method of locking the converter station will be adopted, but the overcurrent may continue to flow in the diode in the sub-module. The converter station overcurrent protection strategy adopted in this paper is to prevent the overcurrent from flowing through the continuation diode and to achieve overcurrent protection for the sub-module. Therefore, a thyristor K2 with greater current capacity is applied in parallel at the output end of the sub-module. As shown in Figure 11 below.

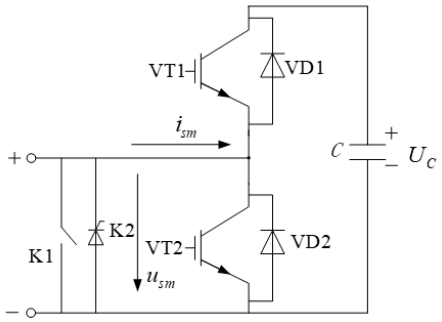

Figure 11. Overcurrent protection device.

Table 3 shows the working state and current path of the sub-module. When the MMC-HVDC system works normally, the thyristor K2 is in the off state. However, when the MMC-HVDC system is in a normal working state, the thyristor K2 is in an off state. However, when the signal detection device of the system detects that the bridge arm current overflows and exceeds the set margin, the system will immediately lock the converter and trigger the conduction of the thyristor K2. Because K2 has a stronger flow capacity, most of the current flow through K2, protecting the diode. In general, if the fault is determined to be instantaneous through signal detection, and the fault that generates overcurrent is cleared, the converter station will be restarted after the converter is locked for some time so that it will gradually return to the original normal operation and working state. If the fault is not rectified, the overcurrent protection is still enabled and the system is locked for some time. If the system fails to restart, the system will restart several times according to the present times within the specified number of times. If the startup is not successful, the circuit breaker on the AC side will be opened and the system will exit.

Table 3. Redundant sub-module working status and current path.

Working Status of the Sub-Module	Switch State	Current Path
Hot standby	K1 broken VT1 broken VT2 open	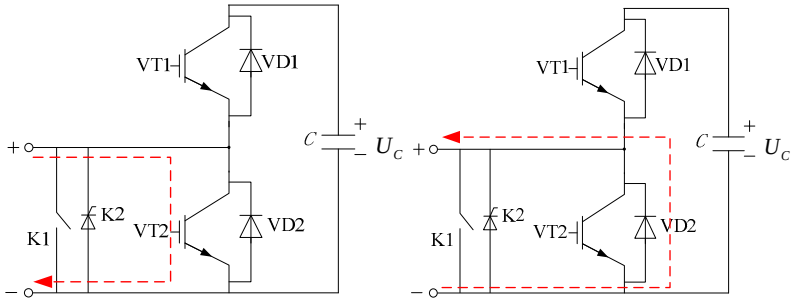
Cold standby	K1 closed VT1 Shut off VT2 Shut off	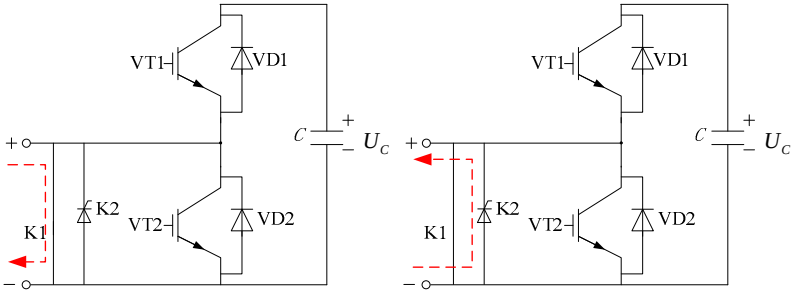

4. Conclusions

In the summary section, starting with the modular multilevel converter sub-module, the protection strategy of sub-module redundancy is discussed, and the AC side fault of the protection modular multilevel converter outlined in this chapter mainly studies the internal faults of the converter station. First, the sub-module of MMC-HVDC converter station system failure reasons are analyzed, in terms of protecting the normal operation of the whole system. We put forward the setting a certain number of hot standby modules and cold standby modules at the end of each bridge arm. According to the number of sub-modules of the failure of a relationship with the number of redundant sub-modules, we propose the corresponding module redundancy protection strategy. The strategy of adding redundant sub-modules proposed in this paper has a good effect. Secondly, the reasons for the failure of the bridge arm reactor in the converter station of the MMC-HVDC system are analyzed in detail, the change of inductance value caused by the reactor failure is simulated, and the corresponding solutions are put forward. Aiming at the overcurrent phenomenon caused by the fault of the converter station, the thyristor with stronger conduction ability is put forward in the sub-module to protect the switching device and maintain the normal operation of the system.

Author Contributions: Conceptualization, C.Z. and M.L.; Funding acquisition, Y.Z. and M.L.; Investigation, C.Z., S.J., Y.X. and L.W.; Methodology, C.Z., L.W. and M.L.; Project administration, C.Z., Y.Z. and M.L.; Resources, Y.Z. and M.L.; Software, L.W.; Supervision, Y.Z. and M.L.; Validation, Y.Z.; Visualization, M.L.; Writing—original draft, C.Z. and S.J.; Writing—review & editing, C.Z., S.J., Y.X., D.Z. and Y.M. All authors have read and agreed to the published version of the manuscript.

Funding: This work is supported partially by the National Natural Science Foundation of China (Grant nos. 71974055, and 51772096), Project Supported by Science and Technology Project of SGCC (SGJX0000KXJS1900321), Beijing Science and Technology Project (Z181100005118002), Par-Eu Scholars Program, Science and Technology Beijing 100 Leading Talent Training Project, the Fundamental Research Funds for the Central Universities (2020FR002, 2020MS023, 2020MS028) and the NCEPU "Double First-Class" Program.

Institutional Review Board Statement: In this section, please add the Institutional Review Board Statement and approval number for studies involving humans or animals. Please note that the Editorial Office might ask you for further information. Please add "The study was conducted according to the guidelines of the Declaration of Helsinki, and approved by the Institutional Review Board (or Ethics Committee) of NAME OF INSTITUTE (protocol code XXX and date of approval)." OR "Ethical review and approval were waived for this study, due to REASON (please provide a detailed justification)." OR "Not applicable." for studies not involving humans or animals. You might also choose to exclude this statement if the study did not involve humans or animals.

Informed Consent Statement: Any research article describing a study involving humans should contain this statement. Please add "Informed consent was obtained from all subjects involved in the study." OR "Patient consent was waived due to REASON (please provide a detailed justification)." OR "Not applicable." for studies not involving humans. You might also choose to exclude this statement if the study did not involve humans.

Written informed consent for publication must be obtained from participating patients who can be identified (including by the patients themselves). Please state "Written informed consent has been obtained from the patient(s) to publish this paper" if applicable.

Data Availability Statement: In this section, please provide details regarding where data supporting reported results can be found, including links to publicly archived datasets analyzed or generated during the study. Please refer to suggested Data Availability Statements in section "MDPI Research Data Policies" at https://www.mdpi.com/ethics. You might choose to exclude this statement if the study did not report any data.

Acknowledgments: The authors would like to appreciate Meicheng Li and Yan Zhang. Their guidances are of great importance to the successful completion of this study. In addition, we are grateful to each member of the research team.

Conflicts of Interest: The authors declare no conflict of interest. The funders had no role in the design of the study; in the collection, analyses, or interpretation of data; in the writing of the manuscript, or in the decision to publish the results.

References

1. Alam, M.; Abido, M.; Hussein, A.; El-Amin, I. Fault Ride through Capability Augmentation of a DFIG-Based Wind Integrated VSC-HVDC System with Non-Superconducting Fault Current Limiter. *Sustainability* **2019**, *11*, 1232.
2. Xue, S.; Lu, J.; Sun, Y.; Wang, S.; Li, B. A reverse travelling wave differential protection scheme for DC lines in MMC–HVDC system with metallic return. *Int. J. Electr. Power Energy Syst.* **2022**, *135*, 107521.
3. Yang, S.; Xiang, W.; Li, R.; Lu, X.; Wen, J. An Improved DC fault Protection Algorithm for MMC HVDC Grids based on Modal Domain Analysis. *IEEE J. Emerg. Sel. Top. Power Electron.* **2019**, *8*, 4086–4099.
4. Li, Z.; Ping, W.; Zhu, H.; Chu, Z.; Li, Y. An Improved Pulse Width Modulation Method for Chopper-Cell-Based Modular Multilevel Converters. *IEEE Trans. Power Electron.* **2012**, *27*, 3472–3481.
5. Alsokhiry, F.; Adam, G.P. Multi-Port DC-DC and DC-AC Converters for Large-Scale Integration of Renewable Power Generation. *Sustainability* **2020**, *12*, 8440.
6. Xue, S.; Gu, C.; Liu, B.; Fan, B. Analysis and Protection Scheme of Station Internal AC Grounding Faults in a Bipolar MMC-HVDC System. *IEEE Access* **2020**, *8*, 26536–26548.
7. Tan, X.; Ren, L.; Tang, Y.; Shi, J.; Li, Z. Analysis of R-SFCL with Shunt Resistor in MMC-HVDC System using novel R-Q method. *IEEE Trans. Appl. Supercond.* **2020**, *30*, 5601405.
8. Zhou, J.; Wei, J.; Xie, G.; Ran, L.; Zhang, Y. Architecture Design of Digital Twin Platform for AC&DC Hybrid Transmission System with MMC-HVDC. *J. Phys. Conf. Ser.* **2021**, *1754*, 12041–12047.
9. Mohammadi, F.; Nazri, G.; Saif, M. A new topology of a fast proactive hybrid DC circuit breaker for MT-HVDC grids. *Sustainability* **2019**, *11*, 4493.
10. Darbas, C.; Olivier, J.C.; Ginot, N.; Poitiers, F.; Batard, C. Cascaded Smart Gate Drivers for Modular Multilevel Converters Control: A Decentralized Voltage Balancing Algorithm. *Energies* **2021**, *14*, 3589.
11. Qoria, T.; Guillaud, X. Control of power electronics-driven power sources. In *Converter-Based Dynamics and Control of Modern Power Systems*; Elsevier: Amsterdam, The Netherlands, 2021.
12. Chen, Z.; Yan, J.; Lu, C. Coordinated Control between Prevention and Correction of AC/DC Hybrid Power System Based on Steady-state Security Region. *IEEE Access* **2021**, *9*, 47842–47855.
13. Laha, P.; Chakraborty, B. Cost optimal combinations of storage technologies for maximizing renewable integration in Indian power system by 2040: Multi-region approach. *Renew. Energy* **2021**, *179*, 233–247.
14. Vozikis, D.; Psaras, V.; Alsokhiry, F.; Adam, G.; Al-Turki, Y. Customized converter for cost-effective and DC-fault resilient HVDC Grids. *Int. J. Electr. Power Energy Syst.* **2021**, *131*, 107038.

15. Stefani, A.; Yazidi, A.; Rossi, C.; Filippetti, F.; Casadei, D.; Capolino, G.A. Doubly Fed Induction Machines Diagnosis Based on Signature Analysis of Rotor Modulating Signals. *IEEE Trans. Ind. Appl.* **2008**, *44*, 1711–1721.
16. Nandi, A.K.; Wang, Q.; Yu, Y.; Darwish, M.; Ahmed, H.O. Fault Detection and Classification in MMC-HVDC Systems Using Learning Methods. Sensors **2020**, *20*, 4438.
17. Skinner, B.; Mancarella, P.; Vrakopoulou, M.; Hiskens, I. Incorporating new power system security paradigms into low-carbon electricity markets. *Electr. J.* **2020**, *33*, 106837.
18. Khorasaninejad, M.; Radmehr, M.; Firouzi, M.; Koochaki, A. Application of a resistive mutual-inductance fault current limiter in VSC-based HVDC system. *Int. J. Electr. Power Energy Syst.* **2022**, *134*, 107388.
19. Ghadi, R.J.; Mehrasa, M.; Adabi, M.E.; Bacha, S. Lyapunov theory-based control strategy for multi-terminal MMC-HVDC systems. *Int. J. Electr. Power Energy Syst.* **2021**, *129*, 106778.
20. Xia, X.; Xu, L.; Zhao, X.; Zeng, X.; Yi, H. Modular multilevel converter predictive control strategy based on energy balance. *J. Power Electron.* **2021**, *21*, 757–767.
21. Rodriguez, J.; Franquelo, L.G.; Kouro, S.; Leon, J.I.; Portillo, R.C.; Prats, M.; Perez, M.A. Multilevel Converters: An Enabling Technology for High-Power Applications. *Proc. IEEE* **2009**, *97*, 1786–1817.
22. Mukherjee, D.; Chakraborty, S.; Ghosh, S. Power system state forecasting using machine learning techniques. *Electr. Eng.* **2021**, *104*, 283–305.
23. Gemmell, B. Prospects of multilevel VSC technologies for power transmission. In Proceedings of the 2008 IEEE/PES Transmission and Distribution Conference and Exposition, Chicago, IL, USA, 21–24 April 2008.
24. Wu, J.Y.; Lan, S.; Xiao, S.J.; Yuan, Y.B. Single Pole-to-ground Fault Location System for MMC-HVDC Transmission Lines Based on Active Pulse and CEEMDAN. *IEEE Access* **2021**, *9*, 42226–42235.
25. Zhou, G.; Han, M.; Filizadeh, S.; Cao, X.; Huang, W. Studies on the combination of RSFCLs and DCCBs in MMC-MTDC system protection. *Int. J. Electr. Power Energy Syst.* **2021**, *125*, 106532.
26. Song, Q.; Liu, W.; Li, X.; Rao, H.; Xu, S.; Li, L. A Steady-State Analysis Method for a Modular Multilevel Converter. *IEEE Trans. Power Electron.* **2013**, *28*, 3702–3713.
27. Li, X.; Song, Q.; Liu, W.; Rao, H.; Xu, S.; Li, L. Protection of Nonpermanent Faults on DC Overhead Lines in MMC-Based HVDC Systems. *IEEE Trans. Power Deliv.* **2013**, *28*, 483–490.
28. Guan, M.; Xu, Z.; Li, H. Analysis of DC voltage ripples in modular multilevel converters. In Proceedings of the IEEE 2010 International Conference on Power System Technology, Zhejiang, China, 24–28 October 2010; pp. 1–6.
29. Yuebin, Z.; Daozhuo, J.; Jie, G.; Pengfei, H.; Zhiyong, L. Control of Modular Multilevel Converter Based on Stationary Frame under Unbalanced AC System. In Proceedings of the IEEE 2012 Third International Conference on Digital Manufacturing & Automation, Guilin, China, 31 July–2 August 2012; pp. 293–296.
30. Tu, Q.; Xu, Z.; Chang, Y.; Guan, L. Suppressing DC Voltage Ripples of MMC-HVDC under Unbalanced Grid Conditions. *IEEE Trans. Power Deliv.* **2012**, *27*, 1332–1338.
31. Guan, M.; Xu, Z. Modeling and Control of a Modular Multilevel Converter-Based HVDC System Under Unbalanced Grid Conditions. *IEEE Trans. Power Electron.* **2012**, *27*, 4858–4867.
32. Adam, G.P.; Anaya-Lara, O.; Burt, G.; Finney, S.J.; Williams, B.W. Comparison between Two VSC-HVDC Transmission Technologies: Modular and Neutral Point Clamped Multilevel Converter. In Proceedings of the IEEE 35th Annual Conference of the IEEE Industrial Electronics Society, *Porto*, *Portugal*, 3–5 November 2009; pp. 1–4.
33. Li, R.; Fletcher, J. AC Voltage Control of DC/DC Converters Based on Modular Multilevel Converters in Multi-Terminal High-Voltage Direct Current Transmission Systems. *Energies* **2016**, *9*, 1064.
34. Schmitt, D.; Wang, Y.; Weyh, T.; Marquardt, R. DC-side Fault Curret Management in Extended Multiterminal- HVDC-Grids. In Proceedings of the 9th International Multi-Conference on Systems, Signals and Devices, Chemnitz, Germany, 20–23 March 2012; pp. 1–5.
35. Miyara, R.; Nakadomari, A.; Matayoshi, H.; Takahashi, H.; Hemeida, A.M.; Senjyu, T. A Resonant Hybrid DC Circuit Breaker for Multi-Terminal HVDC Systems. *Sustainability* **2020**, *12*, 7771.
36. Fu, Z.; Sima, W.; Yang, M.; Sun, P.; Yuan, T.; Wang, X.; Long, Y. A Mutual-Inductance-Type Fault Current Limiter in MMC-HVDC Systems. *IEEE Trans. Power Deliv.* **2020**, *35*, 2403–2413. https://doi.org/10.1109/TPWRD.2020.2967837.
37. Tahir, M.; Hu, S.; Meng, Y. Unit Partition Resonance Analysis Strategy for Impedance Network in Modular Power Converters. *Front. Energy Res.* **2022**, *10*, 1–12. https://doi.org/10.3389/fenrg.2022.823938.
38. Ahmed, H.; Nandi, A.K. Three-Stage Hybrid Fault Diagnosis for Rolling Bearings with Compressively Sampled Data and Subspace Learning Techniques. *IEEE Trans. Ind. Electron.* **2019**, *66*, 5516–5524.
39. Zhang, Y.; Tang, F.; Qin, F.; Li, Y.; Gao, X.; Du, N. Research on Dynamic Reactive Power Compensation Scheme for Inhibiting Subsequent Commutation Failure of MIDC. *Sustainability* **2021**, *13*, 7829.
40. Katyara, S.; Hashmani, A.; Chowdhary, B.S.; Musavi, H.A.; Aleem, A.; Chachar, F.A.; Shah, M.A. Wireless Networks for Volt age Stability Analysis and Anti-islanding Protection of Smart Grid System. *Wirel. Pers. Commun.* **2021**, *116*, 1361–1378.
41. Zhang, Y.; Wang, S.; Liu, T.; Zhang, S.; Lu, Q. A traveling-wave-based protection scheme for the bipolar voltage source converter based high voltage direct current (VSC-HVDC) transmission lines in renewable energy integration. *Energy* **2021**, *216*, 119312.
42. Hossain, M.I.; Abido, M.A. SCIG Based Wind Energy Integrated Multiterminal MMC-HVDC Transmission Network. *Sustainability* **2020**, *12*, 3622.